

Convergence of Godunov-Type Schemes for Scalar Conservation Laws under Large Time Steps¹

Jing-Mei Qiu² and Chi-Wang Shu³

Division of Applied Mathematics, Brown University, Providence, Rhode Island 02912

Abstract

In this paper, we consider convergence of classical high order Godunov-type schemes towards entropy solutions for scalar conservation laws. It is well known that sufficient conditions for such convergence include total variation boundedness of the reconstruction and cell or wavewise entropy inequalities. We prove that under large time steps, we only need total variation boundedness of the reconstruction to guarantee such convergence. We discuss high order total variation bounded reconstructions to fulfill this sufficient condition and provide numerical examples on one dimensional convex conservation laws to assess the performance of such large time step Godunov-type methods. To demonstrate the generality of this approach, we also prove convergence and give numerical examples for a large time step Godunov-like scheme involving Sanders' third order total variation diminishing reconstruction using both cell averages and point values at cell boundaries.

Keywords: hyperbolic conservation laws; Godunov-type scheme; high order accuracy; total variation diminishing; total variation bounded; convergence; entropy solution

¹Research supported by ARO grant W911NF-04-1-0291, NSF grant DMS-0510345 and AFOSR grant FA9550-05-1-0123.

²E-mail: jqiu@dam.brown.edu

³E-mail: shu@dam.brown.edu

1 Introduction

In this paper, we consider the Cauchy problem of the scalar conservation law:

$$\begin{cases} u_t + \nabla \cdot f(u) = 0, & \text{in } \mathbb{R}^m \times [0, T] \\ u(x, 0) = u_0(x), & \text{in } \mathbb{R}^m \end{cases} \quad (1.1)$$

where $u_0(x) \in \text{BV}$, the space of functions with bounded variation. We do not consider boundary conditions and assume that the initial condition is either compactly supported or periodic. In most of our presentation we will concentrate on the one dimensional case $m = 1$, and will point out similarities and differences for higher dimensions $m > 1$. The scheme under consideration is the classical Godunov-type scheme, consisting of the following three stages to evolve the cell averages from time level n (denoted by \bar{u}^n) to time level $n + 1$ (denoted by \bar{u}^{n+1}):

1. *Reconstruction*: obtain a high order piecewise polynomial reconstruction $u^n(x)$ whose cell averages agree with the given cell averages \bar{u}^n . We denote this reconstruction operator as $Re(\bar{u}^n)$.
2. *Evolution*: evolve $u^n(x)$ by the conservation law (1.1) *exactly* for a time step Δt , to obtain a solution $\tilde{u}^{n+1}(x)$ which is in general *not* piecewise polynomial anymore. We denote this evolution operator as $S_{\Delta t}(u^n)$.
3. *Averaging*: average the function $\tilde{u}^{n+1}(x)$ to obtain the cell averages \bar{u}^{n+1} at time level $n + 1$. We denote this averaging operator as $A(\tilde{u}^{n+1})$.

The Godunov-type scheme, using the notations introduced above, can be described abstractly as

$$\begin{cases} \bar{u}^0 = A(u_0) \\ \bar{u}^{n+1} = A \circ S_{\Delta t} \circ Re(\bar{u}^n), & n = 0, 1, \dots, N - 1. \end{cases} \quad (1.2)$$

The purpose of the reconstruction step is to increase the formal accuracy of the scheme. It is usually achieved by using cell averages of several neighboring cells to obtain a high order reconstructed polynomial. In order to be more specific, let us first introduce some notations.

For example, in the one dimensional case, the mesh is given by $I_j = [x_{j-\frac{1}{2}}, x_{j+\frac{1}{2}}]$. The center of the cell I_j is given by $x_j = \frac{1}{2} (x_{j-\frac{1}{2}} + x_{j+\frac{1}{2}})$, and the size of the cell I_j is denoted by $\Delta x = x_{j+\frac{1}{2}} - x_{j-\frac{1}{2}}$, which is considered to be a constant (uniform mesh) in this paper for simplicity of notations. The cell average of a function $u(x)$ in the cell I_j is defined as

$$\bar{u}_j = A(u)_j = \frac{1}{\Delta x} \int_{x_{j-\frac{1}{2}}}^{x_{j+\frac{1}{2}}} u(x) dx$$

A second order reconstruction would be a piecewise linear function, and the linear reconstruction $p_j(x)$ in cell I_j could be the unique linear polynomial satisfying

$$\frac{1}{\Delta x} \int_{x_{j-\frac{3}{2}}}^{x_{j-\frac{1}{2}}} p_j(x) dx = \bar{u}_{j-1}, \quad \frac{1}{\Delta x} \int_{x_{j-\frac{1}{2}}}^{x_{j+\frac{1}{2}}} p_j(x) dx = \bar{u}_j,$$

namely, $p_j(x)$ agrees with the given cell averages of $u(x)$ over the two cells $\{I_{j-1}, I_j\}$, which is called the *stencil* of the reconstruction $p_j(x)$. Usually, we require that the stencil for the reconstruction in cell I_j contains at least I_j itself. Additional cells in the stencil can be chosen according to symmetry or stability (non-oscillation) considerations. For example, the stencil for the linear polynomial $p_j(x)$ above could also be $\{I_j, I_{j+1}\}$, which would of course produce a different reconstructed linear polynomial.

The reconstruction is called (formally) k -th order accurate, namely

$$|Re(\bar{u})(x) - u(x)| \leq C\Delta x^k, \quad x \in I_j \tag{1.3}$$

if the reconstructed polynomial in I_j is $(k-1)$ -th degree with a stencil of k cells over which the function $u(x)$ is smooth. Here and below C (or \tilde{C}) will denote a generic constant independent of the mesh sizes Δx and Δt , which may have different values in different locations. For more details of second and higher order reconstructions, we refer to [11, 18].

A reconstruction is called total variation bounded (TVB) if

$$TV(Re(\bar{u})) \leq (1 + C\Delta x)TV(\bar{u}) \tag{1.4}$$

and it is called total variation diminishing (TVD) if (1.4) holds with $C = 0$. Here the total variation of a piecewise smooth function $g(x)$ is defined as usual

$$TV(g) = \int |g'(x)| dx$$

and the total variation of \bar{u} in (1.4) is defined with \bar{u} considered as a piecewise constant function.

Since the exact evolution operator $S_{\Delta t}$ and the averaging operator A do not increase the total variation of a function, the total variation of the final solution \bar{u}^N of the Godunov-type scheme at a fixed time $T = N\Delta t$, is bounded by a constant C independent of the mesh sizes Δx and Δt , when both of them go to zero, if the reconstruction is TVB. This constant C is the total variation of the initial data if the reconstruction is TVD.

By compactness, the sequence of numerical solutions of a Godunov-type scheme with a TVB reconstruction, when the mesh sizes Δx and Δt both go to zero, has a convergent subsequence in L^1 . Since the scheme is conservative, the limit of such a convergent subsequence is a weak solution to (1.1). However, because of the non-uniqueness of weak solutions, we cannot conclude the convergence of the original sequence of numerical solutions, nor can we claim that the limit of a convergent subsequence is the physically relevant entropy solution. Typically, we would need an additional cell entropy inequality, e.g. [15], or a wavewise entropy inequality, e.g. [21], to imply such convergence. Such cell or wavewise entropy inequalities are very difficult to obtain for high order schemes, especially for non-convex conservation laws for which such entropy inequalities are needed for all entropies rather than just for one of them. As far as we know, within self-similar finite difference or finite volume framework, such cell or wavewise entropy inequalities have been obtained only for second order MUSCL type schemes for scalar one dimensional convex conservation laws [15, 21], and for a special second order scheme for general conservation laws which evolves cell averages and cell slopes independently [1]. These schemes are all explicit schemes with the usual CFL restriction $\Delta t = O(\Delta x)$. It seems that for such situation a cell or wavewise entropy inequality is necessary for convergence towards entropy solutions, see for example [15] in which it is proven that finite volume schemes (those which evolve only cell averages and rely on reconstruction to achieve higher order accuracy) which satisfy all entropy conditions are necessarily only first order accurate, and [20] in which a counter example is shown

to demonstrate that second order TVD Godunov-type scheme can converge to an entropy violating solution for non-convex conservation laws. We remark that cell entropy inequality for the square entropy can be obtained in more general situations (arbitrary order of accuracy, general triangulation in multi-space dimensions, arbitrary scalar conservation laws) for the semi-discrete discontinuous Galerkin method [7], but this is a totally different class of schemes in which no reconstruction is involved and the complete polynomial within a cell is evolved in time to obtain high order accuracy.

We now mention a few papers in the literature which directly motivated our work in this paper. Lions and Souganidis [13] proved the convergence of an implicit MUSCL scheme to the entropy solution of strictly convex scalar one dimensional Hamilton-Jacobi equation and conservation law under a large time step assumption, namely $\Delta x = o(\Delta t)$. For one dimensional convex Hamilton-Jacobi equations, which are very closely related to conservation laws (1.1), Ferretti [3] proved the convergence of a semi-Lagrangian scheme to the viscosity solution (the corresponding solution to the entropy solution for conservation laws), again under a large time step assumption $\Delta x = o(\Delta t)$. This convergence holds for quite general high order reconstructions, e.g. the ENO reconstruction [6] up to fifth order and WENO reconstruction [8] up to ninth order, see [3, 2]. The message in [13, 3, 2] seems to be that it is easier to prove convergence for large time step ($\Delta x = o(\Delta t)$) schemes. Of course, such choice of the time step violates the traditional CFL condition for local explicit schemes. One would need either to take implicit time discretization, as in [13], or semi-Lagrangian time discretization, namely following the characteristics, as in [3, 2].

In this paper we prove that, indeed, the large time step assumption $\Delta x = o(\Delta t)$ allows us to bypass the verification of cell or wavewise entropy conditions and prove the convergence towards the entropy solution of Godunov-type schemes solely under the assumption of a TVB reconstruction, for general scalar conservation laws (1.1). Since self-similar TVB reconstruction is available in one dimension to third order accuracy [12], we then have third order accurate Godunov-type schemes in one dimension which can be proven con-

vergent towards the entropy solution. Of course, to actually implement the large time step Godunov-type schemes is not trivial. We discuss an effective implementation, similar to the semi-Lagrangian scheme in [3, 2] for Hamilton-Jacobi equations, for one dimensional scalar convex conservations.

The paper is organized as follows. Section 2 contains our main convergence result and its proof. In section 3, the TVB property of the numerical solution is considered. Examples of high order TVB reconstruction are given. Section 4 discusses an effective implementation of the large time step Godunov-type scheme for one dimensional scalar convex conservation laws and provides numerical results verifying the performance of such schemes. In order to demonstrate the generality of this approach, we consider in section 5 a Godunov-like scheme using a third order TVD reconstruction due to Sanders [16], which uses both cell averages and point values at cell boundaries for the reconstruction and does not exactly fit our large time step Godunov-type scheme framework, but the convergence can be obtained along similar lines. Concluding remarks are given in section 6.

2 Convergence of large time step Godunov-type schemes

We consider the Godunov-type scheme (1.2) for solving the scalar conservation law (1.1), under the following three assumptions:

1. The reconstruction operator Re satisfies

$$\|\bar{u} - Re(\bar{u})\|_{L^1} \leq C \Delta x TV(\bar{u}) \quad (2.1)$$

for any piecewise constant function \bar{u} ;

2. The total variation of the numerical solution is uniformly bounded

$$TV(\bar{u}^n) \leq C \quad (2.2)$$

for all mesh sizes Δx and Δt satisfying $n\Delta t \leq T$;

3. Large time step condition

$$\lim_{\Delta x \rightarrow 0} \frac{\Delta x}{\Delta t} = 0 \quad (2.3)$$

We have the following convergence result under these assumptions.

Theorem 2.1. The numerical solution of the Godunov-type scheme (1.2) for solving the scalar conservation law (1.1) converges in L^1 to the entropy solution of (1.1) when the mesh size Δx goes to zero, if the three assumptions (2.1), (2.2) and (2.3) are satisfied.

Proof: We denote the exact entropy solution of (1.1) at time level t^n by $u(\cdot, t^n)$ and the L^1 difference between this exact solution and the reconstructed numerical solution $u^n = Re(\bar{u}^n)$ at time level t^n by e^n :

$$e^n = \|u(\cdot, t^n) - Re(\bar{u}^n)\|_{L^1}. \quad (2.4)$$

First, we notice that

$$\begin{aligned} \|A(u(\cdot, t^n)) - \bar{u}^n\|_{L^1} &= \|A(u(\cdot, t^n)) - A \circ S_{\Delta t} \circ Re(\bar{u}^{n-1})\|_{L^1} \\ &= \|A(u(\cdot, t^n) - S_{\Delta t} \circ Re(\bar{u}^{n-1}))\|_{L^1} \\ &\leq \|u(\cdot, t^n) - S_{\Delta t} \circ Re(\bar{u}^{n-1})\|_{L^1} \\ &= \|S_{\Delta t}(u(\cdot, t^{n-1})) - S_{\Delta t} \circ Re(\bar{u}^{n-1})\|_{L^1} \\ &\leq \|u(\cdot, t^{n-1}) - Re(\bar{u}^{n-1})\|_{L^1} = e^{n-1} \end{aligned} \quad (2.5)$$

where the third inequality is due to the fact that the averaging operator A does not increase the L^1 norm of a function, and the fifth inequality is due to the L^1 contraction property of the exact entropy solution operator $S_{\Delta t}$ of (1.1) [10]. Also for a bounded variation function w , it is easy to verify that

$$\|w - A(w)\|_{L^1} \leq C\Delta x TV(w) \quad (2.6)$$

In fact, for the one dimensional case

$$\begin{aligned}
\|w - A(w)\|_{L^1} &= \sum_j \int_{I_j} |w(x) - \bar{w}_j| dx = \sum_j \int_{I_j} |w(x) - w(\bar{x}_j)| dx \\
&= \sum_j \int_{I_j} \left| \int_{\bar{x}_j}^x w'(\xi) d\xi \right| dx \leq \sum_j \int_{I_j} \int_{I_j} |w'(\xi)| d\xi dx \\
&= \Delta x \sum_j \int_{I_j} |w'(\xi)| d\xi = \Delta x TV(w)
\end{aligned}$$

where we have used the mean value theorem to conclude that the cell average \bar{w}_j equals $w(\bar{x}_j)$ for some point \bar{x}_j inside I_j , which is valid if $w(x)$ is continuous inside I_j . However, (2.6) is valid also when $w'(x)$ contains δ -functions, as long as it is of bounded variation. The proof for the multi-dimensional case is similar.

We can now proceed to prove the desired convergence

$$\begin{aligned}
e^n &= \|u(\cdot, t^n) - Re(\bar{u}^n)\|_{L^1} \\
&\leq \|u(\cdot, t^n) - A(u(\cdot, t^n))\|_{L^1} + \|A(u(\cdot, t^n)) - \bar{u}^n\|_{L^1} + \|\bar{u}^n - Re(\bar{u}^n)\|_{L^1} \\
&\leq C\Delta x TV(u(\cdot, t^n)) + e^{n-1} + C\Delta x TV(\bar{u}^n) \\
&\leq \tilde{C}\Delta x + e^{n-1} \\
&\leq \dots \\
&\leq \tilde{C}n\Delta x + e^0 \\
&= \tilde{C}T \frac{\Delta x}{\Delta t} + e^0 \rightarrow 0 \quad \text{as } \Delta x \rightarrow 0
\end{aligned}$$

where for the third inequality we have used (2.6), (2.5) and the assumption (2.1), for the fourth inequality we have used the fact that the exact entropy solution $u(\cdot, t^n)$ is of bounded variation and the assumption (2.2), and for the last limit we have used the large time step assumption (2.3). ■

Next, we prove that the assumption (2.1) is satisfied by all commonly used reconstructions, including the high order ENO and WENO reconstructions [6, 8]. As before, for simplicity we divide the computational domains into uniform cells (in one dimension these

are non-overlapping intervals of the same length Δx covering the whole computational domain). We require the reconstruction to be a piecewise polynomial function, namely it is a polynomial over each cell I_j . The reconstructed polynomial in I_j is uniquely determined by requiring that it has the same cell average as the given one over each cell in a stencil, which is a set of finitely many cells (the number of cells in this set is fixed and does not depend on the mesh size Δx) and contains the given cell I_j . For such reconstructions we have the following result.

Lemma 2.2. The assumption (2.1) is satisfied by any piecewise polynomial reconstruction with a local stencil containing finitely many cells.

Proof: We prove this lemma for the one dimensional case. The proof for the multi-dimensional case is similar. Assume the reconstruction stencil for cell I_j is $I_{j-l(j)}, \dots, I_{j+r(j)}$. Since the stencil contains I_j and has only finitely many cells, we have $0 \leq l(j), r(j) \leq M$ for a fixed integer M . The reconstructed polynomial in cell I_j can be written as

$$p(x) = \sum_{i=-l(j)}^{r(j)} p_i \left(\frac{x - x_j}{\Delta x} \right) \bar{u}_{j+i} \quad (2.7)$$

where $p_i(\xi)$ are polynomials independent of Δx and the location I_j , see for example [18] for the explicit expression of $p_i(\xi)$. We therefore have $|p_i(\xi)| \leq C$ for some constant C when ξ is in the relevant range $|\xi| \leq \frac{1}{2}$. Also, by consistency (i.e. the reconstruction is exact if $\bar{u}_j \equiv 1$), we have

$$\sum_{i=-l(j)}^{r(j)} p_i \left(\frac{x - x_j}{\Delta x} \right) = 1$$

Hence

$$p(x) - \bar{u}_j = \sum_{i=-l(j)}^{r(j)} p_i \left(\frac{x - x_j}{\Delta x} \right) (\bar{u}_{j+i} - \bar{u}_j)$$

We now have

$$\begin{aligned}
\|\bar{u} - Re(\bar{u})\|_{L^1} &= \sum_j \|\bar{u} - Re(\bar{u})\|_{L^1(I_j)} \\
&= \sum_j \int_{I_j} \left| \sum_{i=-l(j)}^{r(j)} p_i \left(\frac{x - x_j}{\Delta x} \right) (\bar{u}_{j+i} - \bar{u}_j) \right| dx \\
&\leq CM(2M + 1)\Delta x \sum_j |\bar{u}_{j+1} - \bar{u}_j| \\
&= \tilde{C}\Delta x TV(\bar{u})
\end{aligned}$$

■

Clearly, Lemma 2.2 covers both the linear reconstructions, for which the reconstruction stencil relative to I_j is fixed, i.e. $l(j)$ and $r(j)$ do not depend on j , as well as the ENO reconstruction [6], for which the reconstruction stencil depends on the local smoothness of the data \bar{u} . Since the WENO reconstructions [8] are linear combinations of fixed stencil reconstructions with bounded weights (linear combination coefficients, which depend on the local smoothness of the data \bar{u}), Lemma 2.2 also covers WENO reconstructions. Notice that Lemma 2.2 is valid for reconstructions of arbitrarily high order accuracy.

With Lemma 2.2 we obtain the following corollary.

Corollary 2.3. If the reconstruction operator Re is based on piecewise polynomial reconstruction with a local stencil containing finitely many cells, then the numerical solution of the Godunov-type scheme (1.2) for solving the scalar conservation law (1.1) converges in L^1 to the entropy solution of (1.1) when the mesh size Δx goes to zero, if the two assumptions (2.2) and (2.3) are satisfied.

Proof: We would just need to combine the results in Theorem 2.1 and Lemma 2.2. ■

3 TVB property of the numerical solution and examples of the TVB reconstruction operator

The result of the previous section indicates that, apart from the large time step assumption (2.3), which causes difficulties in the actual implementation of the scheme and will be discussed in more detail in next section, we would only need to have a total variation bounded numerical solution to imply convergence. If the reconstruction operator Re is TVB, i.e. it satisfies (1.4), then we easily have

$$\begin{aligned}
 TV(\bar{u}^n) &= TV(A \circ S_{\Delta t} \circ Re(\bar{u}^{n-1})) \\
 &\leq TV(Re(\bar{u}^{n-1})) \\
 &\leq (1 + C\Delta x)TV(\bar{u}^{n-1}) \\
 &\leq \dots \\
 &\leq (1 + C\Delta x)^n TV(\bar{u}^0) \\
 &\leq (1 + C\Delta t)^n TV(u_0) \\
 &\leq e^{CT}TV(u_0)
 \end{aligned}$$

for any n and Δt such that $n\Delta t \leq T$. Here we have used the fact that neither the averaging operator A nor the exact entropy solution evolution operator $S_{\Delta t}$ increases the total variation of a function for the second inequality, and the assumption (2.3) for the sixth inequality (in fact, here we do not need the large time step assumption, we just need the assumption that $\Delta x \leq C\Delta t$). We therefore only need to verify the total variation boundedness of the reconstruction (1.4) in order to guarantee convergence towards entropy solutions for a large time step Godunov-type scheme.

Next we discuss two examples of TVB reconstructions (1.4). We concentrate our attention on self-similar reconstructions, namely reconstructions which do not depend explicitly on the mesh size Δx (see the example of the reconstruction (2.7) in which the polynomials $p_i(\xi)$ do not depend on Δx [18]). In fact, almost all known self-similar TVB reconstructions are

actually TVD. It is very difficult to obtain self-similar TVB reconstructions in two or higher dimensions [4], hence we restrict our attention in one dimension.

1. *Second order MUSCL reconstruction:* This reconstruction [19] is piecewise linear and is second order accurate except at extrema, where it degenerates to first order accuracy. The reconstructed polynomial in cell I_j is given by

$$p(x) = \bar{u}_j + s_j (x - x_j)$$

where the slope s_j is given by

$$s_j = m \left(\frac{\bar{u}_{j+1} - \bar{u}_j}{\Delta x}, \frac{\bar{u}_j - \bar{u}_{j-1}}{\Delta x} \right)$$

with the usual definition of the *minmod* function m [5]

$$m(a, b) = \frac{\text{sign}(a) + \text{sign}(b)}{2} \min(|a|, |b|).$$

In words, the slope is taken as the smaller one (in magnitude) between those of the two reconstruction linear polynomials based on the stencils $\{I_{j-1}, I_j\}$ and $\{I_j, I_{j+1}\}$, unless these two slopes are of opposite sign (i.e. we are at an extremum of the cell average \bar{u}), in which case the slope is taken as zero. This reconstruction is clearly TVD.

2. *Third order non-oscillatory central reconstruction:* This reconstruction [12] is piecewise quadratic and is third order accurate except at extrema, where it degenerates to second order accuracy. The reconstructed polynomial in cell I_j is based on $q_j(x)$, the reconstructed quadratic polynomial over the stencil $\{I_{j-1}, I_j, I_{j+1}\}$, with modification to satisfy a non-oscillatory property (no new extremum) and a maximum principle. The first step is to obtain the non-oscillatory property and is given by

$$p_j^1(x) = \bar{u}_j + \theta_j (q_j(x) - \bar{u}_j) \tag{3.1}$$

where the limiter θ_j is defined as

$$\theta_j = \begin{cases} \min \left(\frac{M_{j+\frac{1}{2}} - \bar{u}_j}{M_j - \bar{u}_j}, \frac{m_{j-\frac{1}{2}} - \bar{u}_j}{m_j - \bar{u}_j}, 1 \right), & \text{if } \bar{u}_{j-1} < \bar{u}_j < \bar{u}_{j+1} \\ \min \left(\frac{M_{j-\frac{1}{2}} - \bar{u}_j}{M_j - \bar{u}_j}, \frac{m_{j+\frac{1}{2}} - \bar{u}_j}{m_j - \bar{u}_j}, 1 \right), & \text{if } \bar{u}_{j-1} > \bar{u}_j > \bar{u}_{j+1} \\ 1, & \text{if } (\bar{u}_{j+1} - \bar{u}_j) (\bar{u}_j - \bar{u}_{j-1}) \leq 0 \end{cases}$$

where

$$M_j = \max_{x \in I_j} q_j(x), \quad m_j = \min_{x \in I_j} q_j(x),$$

$$M_{j \pm \frac{1}{2}} = \max \left(\frac{1}{2}(\bar{u}_j + \bar{u}_{j \pm 1}), q_{j \pm 1}(x_{j \pm \frac{1}{2}}) \right), \quad m_{j \pm \frac{1}{2}} = \min \left(\frac{1}{2}(\bar{u}_j + \bar{u}_{j \pm 1}), q_{j \pm 1}(x_{j \pm \frac{1}{2}}) \right).$$

The second step is to further modify $p_j^1(x)$ to satisfy a maximum principle. If we denote

$$M = \max_{x \in R} u_0(x), \quad m = \min_{x \in R} u_0(x),$$

and

$$M_j^1 = \max_{x \in I_j} p_j^1(x), \quad m_j^1 = \min_{x \in I_j} p_j^1(x),$$

then the final reconstructed polynomial is given by

$$p_j(x) = \begin{cases} \varepsilon^{(1)} (p_j^1(x) - M_j^1) + M, & \text{when } M_j^1 > M \text{ and } m_j^1 \geq m \\ \varepsilon^{(2)} (p_j^1(x) - m_j^1) + m, & \text{when } M_j^1 \leq M \text{ and } m_j^1 < m \\ \varepsilon^{(1)} (p_j^1(x) - M_j^1) + M, & \text{when } \varepsilon^{(1)} < \varepsilon^{(2)}, M_j^1 > M \text{ and } m_j^1 < m \\ \varepsilon^{(2)} (p_j^1(x) - m_j^1) + m, & \text{when } \varepsilon^{(1)} \geq \varepsilon^{(2)}, M_j^1 > M \text{ and } m_j^1 < m \\ p_j^{(1)}(x), & \text{when } M_j^1 \leq M \text{ and } m_j^1 \geq m \end{cases} \quad (3.2)$$

with

$$\varepsilon^{(1)} = \frac{M - \bar{u}_j}{M_j^1 - \bar{u}_j}, \quad \varepsilon^{(2)} = \frac{m - \bar{u}_j}{m_j^1 - \bar{u}_j}.$$

It is proven in [12] that the reconstruction (3.2) is TVB. Moreover, we have

$$\|p_j^1(x) - \bar{u}_j\|_{L^1} = \theta_j \|q_j(x) - \bar{u}_j\|_{L^1},$$

and

$$\|p_j(x) - \bar{u}_j\|_{L^1} = \varepsilon^{(i)} \|p_j^1(x) - \bar{u}_j\|_{L^1}, \quad i = 1, 2 \quad \text{or} \quad \|p_j(x) - \bar{u}_j\|_{L^1} = \|p_j^1(x) - \bar{u}_j\|_{L^1}$$

with $0 \leq \theta_j \leq 1$ and $0 \leq \varepsilon^{(i)} \leq 1$. Therefore,

$$\|p_j(x) - \bar{u}_j\|_{L^1} \leq \|p_j^1(x) - \bar{u}_j\|_{L^1} \leq \|q_j(x) - \bar{u}_j\|_{L^1}.$$

Hence clearly assumption (2.1) is also satisfied by this reconstruction, using Lemma 2.2.

Other possible TVB reconstructions in one dimension include the very high order TVD reconstructions in [14] (however these reconstructions degenerate to first order accuracy at smooth extrema), or the high order TVB reconstructions in [17] (however the reconstructions are no longer self-similar).

4 Implementation of the scheme and numerical examples for one dimensional scalar convex conservation laws

In this section, we discuss a practical implementation of the large time step Godunov-type scheme discussed in the previous section, for one dimensional scalar convex conservation laws, using a semi-Lagrangian type scheme similar to that used in [3, 2] for Hamilton-Jacobi equations.

To implement one time step of the Godunov-type scheme, assume that we have the cell averages \bar{u}^n available, and we apply a reconstruction operator to obtain the reconstruction $u^n(x) = Re(\bar{u}^n)(x)$, which is a piecewise polynomial function. Our job would be to evolve $u^n(x)$ *exactly* for a time step Δt , to obtain a solution $\tilde{u}^{n+1}(x)$, and then take the cell averages of this solution to obtain $\bar{u}^{n+1} = A\tilde{u}^{n+1}$. It is in general very difficult to obtain the solution $\tilde{u}^{n+1}(x)$, especially when Δt is large, however we do not need the details of this solution $\tilde{u}^{n+1}(x)$, only its cell averages $A\tilde{u}^{n+1}$. As demonstrated in Figure 4.1, if we draw a backward characteristic line $\Gamma_{j+\frac{1}{2}}$ from each of the cell boundaries $x_{j+\frac{1}{2}}$ at time level t^{n+1} back to time level t^n with the foot located at $y_{j+\frac{1}{2}}$, such that the entropy solution of (1.1) is a constant $u_{j+\frac{1}{2}}$ along this backward characteristic line $\Gamma_{j+\frac{1}{2}}$, then we can apply the divergence theorem

over the trapezoid region Ω_j to obtain an explicit formula for \bar{u}_j^{n+1} as

$$\begin{aligned} \Delta x \bar{u}_j^{n+1} = & \int_{y_{j-\frac{1}{2}}}^{y_{j+\frac{1}{2}}} u^n(x) dx - \left(\Delta t f \left(u_{j+\frac{1}{2}} \right) + \left(y_{j+\frac{1}{2}} - x_{j+\frac{1}{2}} \right) u_{j+\frac{1}{2}} \right) \\ & + \left(\Delta t f \left(u_{j-\frac{1}{2}} \right) + \left(y_{j-\frac{1}{2}} - x_{j-\frac{1}{2}} \right) u_{j-\frac{1}{2}} \right) \end{aligned} \quad (4.1)$$

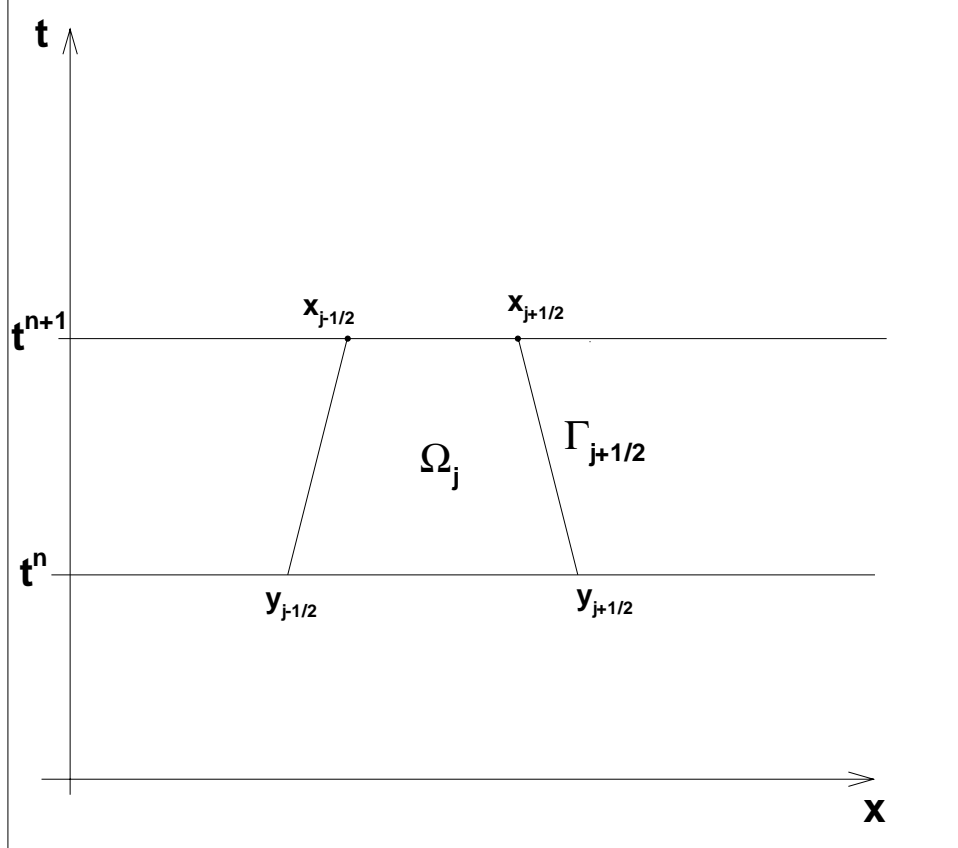


Figure 4.1: The trapezoid region Ω_j in the $x-t$ plane.

Now, the only difficulty left for the implementation of the Godunov-type scheme is to find the backward characteristic lines $\Gamma_{j+\frac{1}{2}}$. Notice that there might be multiple forward characteristic lines from the reconstruction in the previous time level $u^n(x)$ which cross at the target point $(x_{j+\frac{1}{2}}, t^{n+1})$. Even though only one of those characteristic lines (or at most two if the solution happens to be discontinuous at $(x_{j+\frac{1}{2}}, t^{n+1})$) should be correct and the remaining forward characteristic lines will have crossed other characteristic lines before the time t^{n+1} and should be ignored as they are no longer valid after such crossing, it seems difficult to numerically implement the finding of this correct characteristic line with low

computational cost. We have therefore used another strategy to numerically find the correct characteristic line $\Gamma_{j+\frac{1}{2}}$. First, we draw forward characteristic lines for all cell I_i from

$$\left(x_{i-\frac{1}{2}}, u^n \left(x_{i-\frac{1}{2}}^+\right)\right), \quad \left(x_{i+\frac{1}{2}}, u^n \left(x_{i+\frac{1}{2}}^-\right)\right),$$

and (for piecewise polynomials of degree at least 2) from any internal extrema of $u^n(x)$ inside the interval I_i . We denote the left-most and right-most intersections of these characteristic lines with the line $t = t^{n+1}$ as $\xi_{i-\frac{1}{2}}$ and $\xi_{i+\frac{1}{2}}$ respectively, and define

$$J_i = \left[\xi_{i-\frac{1}{2}}, \xi_{i+\frac{1}{2}}\right] \quad (4.2)$$

as the domain of influence of the interval I_i for the time level t^{n+1} . Likewise, we draw the two forward characteristic lines for all cell-boundary points $x_{i+\frac{1}{2}}$ from

$$\left(x_{i+\frac{1}{2}}, u^n \left(x_{i+\frac{1}{2}}^-\right)\right), \quad \left(x_{i+\frac{1}{2}}, u^n \left(x_{i+\frac{1}{2}}^+\right)\right),$$

and denote the left and right intersections of these two characteristic lines with the line $t = t^{n+1}$ as $\eta_{i+\frac{1}{2}}^-$ and $\eta_{i+\frac{1}{2}}^+$ respectively, and define

$$\tilde{J}_{i+\frac{1}{2}} = \left[\eta_{i+\frac{1}{2}}^-, \eta_{i+\frac{1}{2}}^+\right] \quad (4.3)$$

as the domain of influence of the cell-boundary $x_{i+\frac{1}{2}}$ for the time level t^{n+1} . Clearly, because of the convexity of $f(u)$ and hence the monotonicity of $f'(u)$, the sets

$$C_{j+\frac{1}{2}} = \left\{i : x_{j+\frac{1}{2}} \in J_i\right\}, \quad \tilde{C}_{j+\frac{1}{2}} = \left\{i : x_{j+\frac{1}{2}} \in \tilde{J}_{i+\frac{1}{2}}\right\} \quad (4.4)$$

contain all candidate intervals and cell boundary points at time level t^n which will contain forward characteristic lines crossing the target point $(x_{j+\frac{1}{2}}, t^{n+1})$. Furthermore, we can use the minimum and maximum values of $f'(u^n)$ to estimate the largest possible region of dependency for the point $(x_{j+\frac{1}{2}}, t^{n+1})$ at the time level t^n , and search for candidates of the sets $C_{j+\frac{1}{2}}$ and $\tilde{C}_{j+\frac{1}{2}}$ only within this region of dependency to save computational cost. For each J_i with $i \in C_{j+\frac{1}{2}}$, we should be able to find a forward characteristic line from (x_i^*, t^n) , for some point $x_i^* \in I_i$, such that it crosses the target point $(x_{j+\frac{1}{2}}, t^{n+1})$. The

solution $u^* = u^n(x_i^*)$ is a constant along this line, which can be found through the implicit characteristic equation

$$u^* = u^n \left(x_{j+\frac{1}{2}} - f'(u^*) \Delta t \right). \quad (4.5)$$

For the Burgers equations with piecewise polynomial reconstruction of degree no larger than 4, u^* can be obtained analytically. For the general situation a Newton iteration might be needed to find u^* . Likewise, for each $\tilde{J}_{i+\frac{1}{2}}$ with $i \in \tilde{C}_{j+\frac{1}{2}}$, we can find a forward characteristic line from $(x_{i+\frac{1}{2}}, t^n)$ with a solution value u^* between $u^n(x_{i+\frac{1}{2}}^-)$ and $u^n(x_{i+\frac{1}{2}}^+)$, such that it crosses the target point $(x_{j+\frac{1}{2}}, t^{n+1})$. The solution u^* can be found by the the characteristic equation which is simpler than (4.5):

$$f'(u^*) = \frac{x_{j+\frac{1}{2}} - x_{i+\frac{1}{2}}}{\Delta t}. \quad (4.6)$$

Among all the $\{x_i^*, u^*\}$ and $\{x_{i+\frac{1}{2}}, u^*\}$ that we have found, we would need to choose the foot of the correct backward characteristic line $y_{j+\frac{1}{2}}$ according to the classical Lax formula [9]

$$g(y_{j+\frac{1}{2}}) = \min_y g(y) \quad \text{where} \quad g(y) = \int_{-\infty}^y u^n(\xi) d\xi + \Delta t L \left(\frac{x_{j+\frac{1}{2}} - y}{\Delta t} \right) \quad (4.7)$$

where the lower limit $-\infty$ in the integral is irrelevant and can be replaced by any fixed point, and

$$L(v) = \int^v (f')^{-1}(u) du$$

is the Legendre transform of $f(u)$. If there are multiple minimizers to $g(y)$, corresponding to the situation that the solution is discontinuous at $(x_{j+\frac{1}{2}}, t^{n+1})$, then we will just take the smallest minimizer as $y_{j+\frac{1}{2}}$, corresponding to the left limit value of the solution at the discontinuity $(x_{j+\frac{1}{2}}, t^{n+1})$. It is here that we use the property that the conservation law has a convex flux $f(u)$, as the Lax formula is only valid for convex conservation laws.

We now summarize our implementation of the large time step Godunov-type scheme for a scalar one dimensional convex conservation law (1.1), from \bar{u}^n to \bar{u}^{n+1} :

1. Perform a reconstruction to obtain a piecewise polynomial $u^n(x)$.

2. Find the domain of influence J_i for each cell I_i via (4.2) and the domain of influence $\tilde{J}_{i+\frac{1}{2}}$ for each cell boundary point $x_{i+\frac{1}{2}}$ via (4.3).
3. Find the set $C_{j+\frac{1}{2}}$ of all candidate intervals and the set $\tilde{C}_{j+\frac{1}{2}}$ of all candidate cell boundary points at time level t^n which will contain forward characteristic lines crossing the target point $(x_{j+\frac{1}{2}}, t^{n+1})$, via (4.4).
4. For each J_i with $i \in C_{j+\frac{1}{2}}$, find a forward characteristic line from (x_i^*, t^n) with the solution value u^* , via (4.5). Likewise, for each $\tilde{J}_{i+\frac{1}{2}}$ with $i \in \tilde{C}_{j+\frac{1}{2}}$, find a forward characteristic line from $(x_{i+\frac{1}{2}}, t^n)$ with a solution value u^* , via (4.6).
5. Use the Lax formula (4.7) to determine the correct backward characteristic line $\{y_{j+\frac{1}{2}}, u_{j+\frac{1}{2}}\}$ among all the $\{x_i^*, u^*\}$ and $\{x_{i+\frac{1}{2}}, u^*\}$ that we have found above.
6. Use (4.1) to obtain \bar{u}_j^{n+1} for all j .

In the following we provide numerical results of the large time step Godunov-type scheme applied to the Burgers equation, namely (1.1) with $f(u) = \frac{u^2}{2}$, for several different reconstructions and for both smooth and discontinuous solutions. We take $\Delta t = \Delta x^{0.9}$ in all runs.

Example 4.1. Burgers equation with the initial condition

$$u_0(x) = \sin(\pi x), \quad -1 \leq x < 1 \quad (4.8)$$

with periodic boundary condition. The solution at $t = 0.2$ is still smooth and we record the L^1 errors and numerical orders of accuracy in Table 4.1, for the first order Godunov method (no reconstruction), second order MUSCL reconstruction, and third order non-oscillatory reconstruction in [12]. All these cases correspond to TVB reconstructions and hence provable convergence for the large time step Godunov-type scheme according to the discussions in the previous two sections. We can see clearly from Table 4.1 that all schemes achieve their designed order of accuracy.

Table 4.1: L^1 errors and numerical orders of accuracy for different TVD reconstructions. Burgers equation with initial condition (4.8). $t = 0.2$

Number of cells	constant		MUSCL		Liu and Osher	
	L^1 error	order	L^1 error	order	L^1 error	order
34	1.26E-2	–	1.38E-3	–	1.41E-4	–
68	6.30E-3	1.00	2.89E-4	2.26	2.75E-5	2.35
136	3.80E-3	0.72	8.44E-5	1.77	4.38E-6	2.65
272	2.00E-3	0.92	2.66E-5	1.66	5.85E-7	2.90
544	1.06E-3	0.91	7.55E-6	1.81	7.65E-8	2.93
1088	5.33E-4	0.99	1.76E-6	2.09	9.72E-9	2.97

Even though the third order linear central reconstruction (namely the stencil for reconstructing the polynomial in I_j is fixed as $\{I_{j-1}, I_j, I_{j+1}\}$) and the third order ENO reconstruction [6] are not proven TVB, they perform well in this smooth test case, yielding the expected third order accuracy for the large time step Godunov-type scheme, see Table 4.2.

Table 4.2: L^1 errors and numerical orders of accuracy for third order linear central and ENO reconstructions. Burgers equation with initial condition (4.8). $t = 0.2$

Number of cells	central		ENO	
	L^1 error	order	L^1 error	order
34	1.51E-4	–	1.37E-4	–
68	2.65E-5	2.51	2.90E-5	2.24
136	3.86E-6	2.78	5.05E-6	2.52
272	5.21E-7	2.88	6.59E-7	2.93
544	6.79E-8	2.93	9.63E-8	2.77
1088	8.65E-9	2.97	1.21E-8	2.98

Example 4.2. Burgers equation with a discontinuous initial condition

$$u_0(x) = \begin{cases} 1, & \text{if } -1 \leq x < 0 \\ 3, & \text{if } 0 \leq x < 1 \end{cases} \quad (4.9)$$

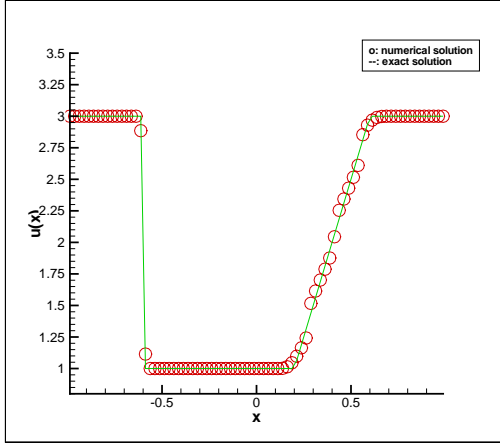
with periodic boundary condition. The solutions of the large time step Godunov-type scheme at $t = 0.2$ for different reconstructions are shown in Figure 4.2. We can see in general good agreement between the numerical and the exact entropy solutions. The first order Godunov

scheme is showing some stair-like features in the rarefaction region, which is well known, and the schemes based on linear reconstructions, namely the second order upwind reconstruction (for this case with $f'(u) > 0$ the stencil for reconstructing the polynomial in I_j is fixed as $\{I_{j-1}, I_j\}$) and the third order central reconstruction are both slightly oscillatory. The schemes based on MUSCL, Liu-Osher non-oscillatory and ENO reconstructions are all non-oscillatory as expected.

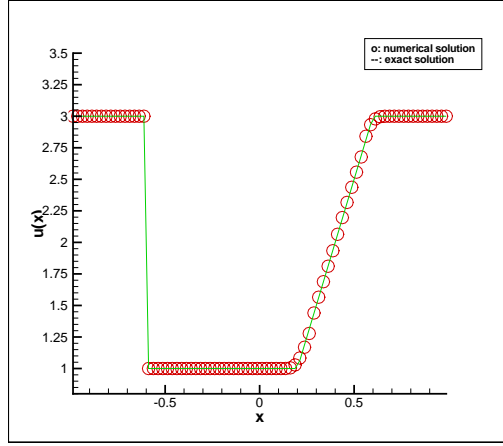
5 Convergence of the large time step Godunov-like scheme based on Sanders' TVD reconstruction

Sanders [16] proposed a third order accurate TVD (he called it total variation non-expansive) scheme by evolving both the cell average and the values at two end points of a cell. He can then obtain a third order TVD scheme instead of the usual Godunov-type TVD scheme which degenerates to second order at best. This scheme does not fit the framework of Godunov-type schemes that we have discussed before, since it evolves not just the cell averages but also point values of the solution at cell boundaries. However, the solution procedure is sufficiently similar to Godunov-type schemes and therefore we will call it a Godunov-like scheme. The scheme is based on a reconstruction operator R_s , which produces a piecewise quadratic function. After a suitable initialization to obtain a piecewise quadratic initial numerical solution $u^0(x)$, the Godunov-type scheme based on Sanders' reconstruction operator R_s can be summarized as:

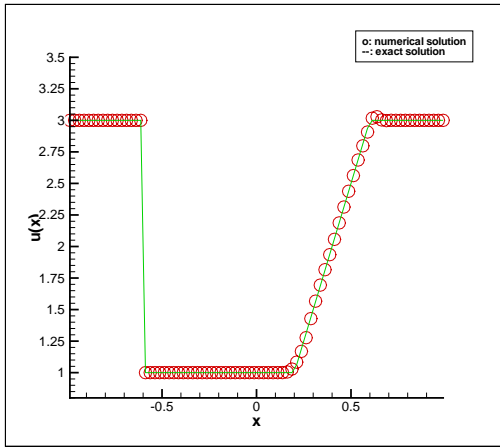
1. *Evolution:* evolve $u^n(x)$ by the conservation law (1.1) *exactly* for a time step Δt , to obtain a solution $\tilde{u}^{n+1}(x)$ which is in general *not* piecewise polynomial anymore. Recall that this evolution operator is denoted as $S_{\Delta t}(u^n)$.
2. *Reconstruction:* obtain a piecewise quadratic polynomial reconstruction $u^n(x)$ by Sanders' reconstruction. We denote this reconstruction operator as $u^{n+1} = R_s(\tilde{u}^{n+1})$.



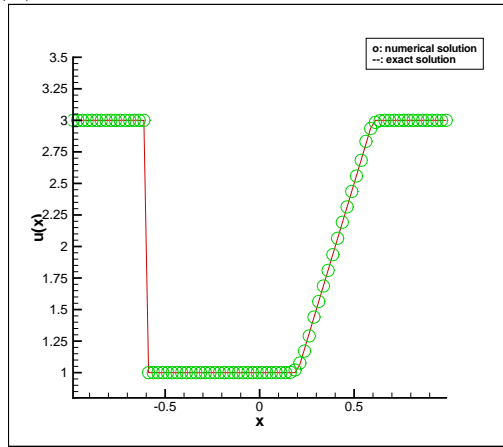
(a)



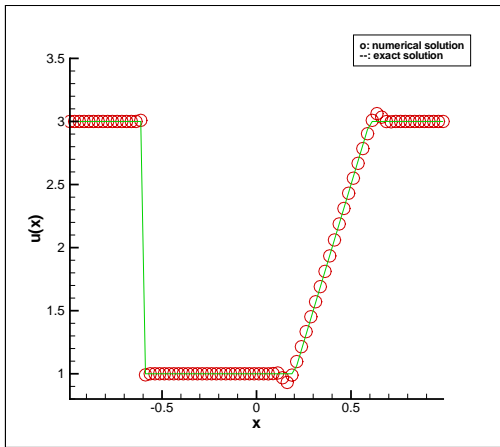
(b)



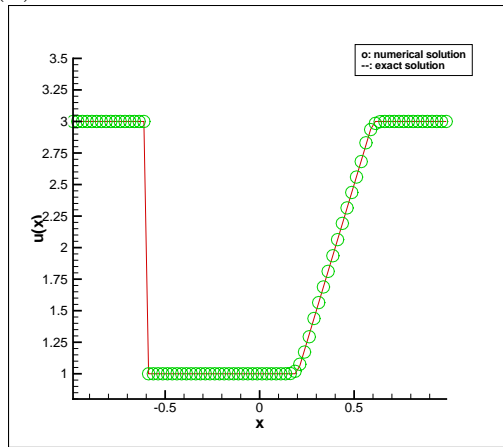
(c)



(d)



(e)



(f)

Figure 4.2: Burgers equation with the discontinuous initial condition (4.9). $t = 0.2$. 80 uniform cells. (a) First order scheme with no reconstruction; (b) second order MUSCL reconstruction; (c) second order upwind reconstruction; (d) third order ENO reconstruction; (e) third order linear central reconstruction; (f) third order non-oscillatory reconstruction of Liu and Osher.

This Godunov-like scheme, using the notations introduced above, can be described abstractly as

$$\begin{cases} u^0 = Rs(u_0) \\ u^{n+1} = Rs \circ S_{\Delta t}(u^n), \quad n = 0, 1, \dots, N-1. \end{cases} \quad (5.1)$$

We will first discuss the TVD reconstruction operator Rs , then prove the convergence of the large time step Godunov-like scheme based on this reconstruction. Finally we will discuss the implementation of this scheme, again for one dimensional scalar convex conservation laws, and provide numerical examples.

5.1 Sanders' TVD reconstruction

Sanders' reconstruction Rs maps a bounded variation function $u(x)$ to a piecewise quadratic polynomial, satisfying the following four properties:

1. Agreement of the cell averages:

$$\int_{I_j} Rs(u)(x) dx = \int_{I_j} u(x) dx, \quad \forall j \quad (5.2)$$

2. TVD:

$$TV(Rs(u)) \leq TV(u) \quad (5.3)$$

3. Maximum (and minimum) principle:

$$\sup Rs(u)(x) \leq \sup u(x), \quad \inf Rs(u)(x) \geq \inf u(x)$$

4. Third order accuracy:

$$Rs(u)(x) = u(x) + O(\Delta x^3)$$

when u is locally smooth.

Let us now describe the details of the reconstruction operator Rs . First, given the cell average \bar{u}_j and the cell boundary values $u_{j-\frac{1}{2}}^+$ and $u_{j+\frac{1}{2}}^-$, we can easily construct a unique quadratic polynomial $q_j(x)$ such that

$$\frac{1}{\Delta x} \int_{x_{j-\frac{1}{2}}}^{x_{j+\frac{1}{2}}} q_j(x) dx = \bar{u}_j, \quad q_j\left(x_{j-\frac{1}{2}}\right) = u_{j-\frac{1}{2}}^+, \quad q_j\left(x_{j+\frac{1}{2}}\right) = u_{j+\frac{1}{2}}^-.$$

In fact, if we denote

$$a = u_{j-\frac{1}{2}}^+ - \bar{u}_j, \quad b = u_{j+\frac{1}{2}}^- - \bar{u}_j, \quad (5.4)$$

then the quadratic polynomial $q_j(x)$ is given by

$$q_j(x) = \hat{q}(a, b)(x) + \bar{u}_j = 3(a+b) \left(\frac{x-x_j}{\Delta x} \right)^2 + (b-a) \left(\frac{x-x_j}{\Delta x} \right) - \frac{1}{4}(a+b) + \bar{u}_j \quad (5.5)$$

We denote M to be the larger one (in magnitude) of a and b and m the smaller one, $\rho = \frac{m}{M}$,

$$E = \begin{cases} \sup_{I_j}(u - \bar{u}_j), & \text{if } M \leq 0 \\ \inf_{I_j}(u - \bar{u}_j), & \text{if } M > 0 \end{cases} \quad (5.6)$$

and $\hat{E} = \frac{E}{M}$. Let

$$\tau_+ = -\hat{E} \cdot \frac{3(1+\rho)}{1+\rho+\rho^2}, \quad \tau_- = -\frac{1}{2} \left((\rho+3\hat{E}) - 3(\hat{E}-\rho)(3\hat{E}+\rho)^{\frac{1}{2}} \right)$$

and

$$\tau_l = \begin{cases} 1, & \text{if } -1 \leq \rho \leq -\frac{1}{2} \\ 1, & \text{if } -\frac{1}{2} < \rho < 0 \text{ and } a = M \\ \min(\tau_-, 1), & \text{if } -\frac{1}{2} < \rho < 0 \text{ and } b = M \\ \min(\tau_+, 1), & \text{if } 0 \leq \rho \leq 1 \end{cases}$$

$$\tau_r = \begin{cases} 1, & \text{if } -1 \leq \rho \leq -\frac{1}{2} \\ 1, & \text{if } -\frac{1}{2} < \rho < 0 \text{ and } b = M \\ \min(\tau_-, 1), & \text{if } -\frac{1}{2} < \rho < 0 \text{ and } a = M \\ \min(\tau_+, 1), & \text{if } 0 \leq \rho \leq 1 \end{cases}$$

then the TVD reconstruction in I_j is defined by

$$Rs(u)(x) = \hat{q}(\tau_l a, \tau_r b)(x) + \bar{u}_j \quad (5.7)$$

with \hat{q} defined in (5.5). It is proved in [16] that the reconstruction Rs is third order accurate and TVD.

5.2 Convergence of the Godunov-like scheme based on Sanders' reconstruction

In this subsection we prove the convergence of the Godunov-like scheme (5.1) based on Sanders' reconstruction.

Theorem 5.1. The numerical solution of the Godunov-like scheme (5.1) with Sanders' reconstruction (5.7) for solving the scalar conservation law (1.1) converges in L^1 to the entropy solution of (1.1) when the mesh size Δx goes to zero, if the large time step assumption (2.3) is satisfied.

Proof: We again denote the exact entropy solution of (1.1) at time level t^n by $u(\cdot, t^n)$ and the L^1 difference between this exact solution and the numerical solution u^n at time level t^n by e^n :

$$e^n = \|u(\cdot, t^n) - u^n\|_{L^1}. \quad (5.8)$$

First, the total variation of the numerical solution is bounded (in fact, diminishing):

$$\begin{aligned} TV(u^n) &= TV(Rs \circ S_{\Delta t}(u^{n-1})) \\ &\leq TV(u^{n-1}) \\ &\leq \dots \\ &\leq TV(u^0) \leq TV(u_0) \end{aligned} \quad (5.9)$$

where we have used the fact that neither the reconstruction operator Rs nor the exact entropy solution evolution operator $S_{\Delta t}$ increases the total variation of a function, for the second inequality.

We now proceed to prove the desired convergence

$$\begin{aligned}
e^n &= \|u(\cdot, t^n) - u^n\|_{L^1} \\
&\leq \|u(\cdot, t^n) - S_{\Delta t}(u^{n-1})\|_{L^1} + \|S_{\Delta t}(u^{n-1}) - A \circ S_{\Delta t}(u^{n-1})\|_{L^1} + \|A \circ S_{\Delta t}(u^{n-1}) - u^n\|_{L^1} \\
&= \|S_{\Delta t}(u(\cdot, t^{n-1})) - S_{\Delta t}(u^{n-1})\|_{L^1} + \|S_{\Delta t}(u^{n-1}) - A \circ S_{\Delta t}(u^{n-1})\|_{L^1} \\
&\quad + \|A \circ Rs \circ S_{\Delta t}(u^{n-1}) - Rs \circ S_{\Delta t}(u^{n-1})\|_{L^1} \\
&\leq \|u(\cdot, t^{n-1}) - u^{n-1}\|_{L^1} + C\Delta x TV(S_{\Delta t}(u^{n-1})) + C\Delta x TV(Rs \circ S_{\Delta t}(u^{n-1})) \\
&\leq e^{n-1} + C\Delta x TV(u^{n-1}) + C\Delta x TV(u^{n-1}) \\
&\leq e^{n-1} + \tilde{C}\Delta x \\
&\leq \dots \\
&\leq \tilde{C}n\Delta x + e^0 \\
&= \tilde{C}T \frac{\Delta x}{\Delta t} + e^0 \rightarrow 0 \quad \text{as } \Delta x \rightarrow 0
\end{aligned}$$

where for the third equality we have used the cell average preserving property (5.2) of Rs ; for the fourth inequality we have used the fact that the exact entropy solution operator $S_{\Delta t}$ is an L^1 contraction, and the inequality (2.6) with $w = S_{\Delta t}(u^{n-1})$ and $w = Rs \circ S_{\Delta t}(u^{n-1})$ respectively; for the fifth inequality we have used the fact that the reconstruction operator Rs and the exact entropy solution operator $S_{\Delta t}$ are both TVD; and for the sixth inequality we have used the fact that the total variation of the numerical solution is bounded (5.9). ■

5.3 Implementation and numerical examples

For one dimensional scalar convex conservation law (1.1), the implementation of the large time step Godunov-like scheme based on Sanders' reconstruction operator Rs is similar to that for the large time step Godunov-type scheme described in detail in section 4. This is because the procedure described in section 4 provides both the cell average \bar{u}_j^{n+1} and the cell boundary values $u_{j-\frac{1}{2}}$ and $u_{j+\frac{1}{2}}$, hence a and b in (5.4) are available. The only additional information needed is the relevant extremum value E in (5.6), which is in general difficult to obtain. We follow Sanders [16] and take instead the corresponding extremum value E

at the previous time level t^n between the feet of the characteristics $y_{j-\frac{1}{2}}$ and $y_{j+\frac{1}{2}}$. This approximation of E is exact if there is no discontinuity within the trapezoid Ω_j (see Figure 4.1), and is over-estimating (larger for the sup and smaller for the inf) if there is at least one shock within Ω_j . It does not affect the accuracy and TVD property of the reconstruction Rs .

In the numerical experiments we take $\Delta t = \Delta x^{0.9}$ as before. We test the large time step Godunov-like scheme based on both a unmodulated third order reconstruction (q_j as given by (5.5)) and on Sanders' TVD reconstruction Rs . We again first test the smooth solution as in Example 4.1. The L^1 errors and numerical orders of accuracy are shown in Table 5.1. We can see clearly third order accuracy for the scheme based on both reconstructions from Table 5.1.

Table 5.1: L^1 errors and numerical orders of accuracy for the third order unmodulated third order reconstruction (5.5) and Sanders' TVD reconstruction Rs . Burgers equation with initial condition (4.8). $t = 0.2$

Number of cells	unmodulated third order		Sanders	
	L^1 error	order	L^1 error	order
40	1.37E-5	–	1.37E-5	–
80	2.26E-6	2.59	2.26E-6	2.59
160	3.64E-7	2.63	3.64E-7	2.63
320	5.12E-8	2.83	5.31E-8	2.77
640	6.70E-9	2.93	6.78E-9	2.97

Next, we test the discontinuous solution as in Example 4.2. Figure 5.1 displays the numerical solution. We can see again good agreement between the numerical and the exact entropy solutions. The scheme based on the unmodulated third order reconstruction is slightly oscillatory, and the scheme based on Sanders' TVD reconstruction is not oscillatory, as expected.

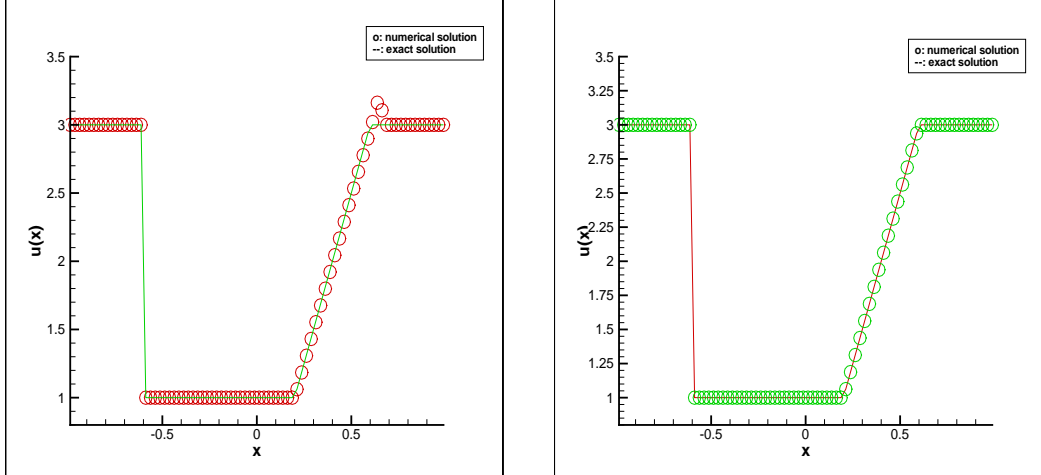


Figure 5.1: Burgers equation with the discontinuous initial condition (4.9). $t = 0.2$. 80 uniform cells. Left: unmodulated third order reconstruction; Right: Sanders' TVD reconstruction.

6 Concluding remarks

The main result of this paper is the proof of convergence towards entropy solutions of large time step Godunov-type schemes with total variation bounded reconstructions for general scalar conservation laws. It is somewhat surprising that no cell or wavewise entropy inequalities are needed in the proof. We have also discussed practical implementation of such large time step Godunov-type schemes for scalar one dimensional convex conservation laws and have provided numerical examples to demonstrate the performance of these schemes. Future work will include investigations on practical implementation for more general equations, and on possible elimination of the total variation bounded assumption on the reconstruction (or the replacement of this condition by a weaker condition easier to satisfy for high order reconstructions in multi-space dimensions).

References

- [1] F. Bouchut, C. Bourdarias and B. Perthame, *A MUSCL method satisfying all the numerical entropy inequalities*, Mathematics of Computation, 65 (1996), pp.1439-1461.

- [2] E. Carlini, R. Ferretti and G. Russo, *A weighted essentially nonoscillatory, large time-step scheme for Hamilton-Jacobi equations*, SIAM Journal on Scientific Computing, 27 (2005), pp.1071-1091.
- [3] R. Ferretti, *Convergence of semi-lagrangian approximation to convex Hamilton-Jacobi equations under (very) large Courant numbers*, SIAM Journal on Numerical Analysis, 40 (2003), pp.2240-2253.
- [4] J. Goodman and R. LeVeque, *On the accuracy of stable schemes for 2D scalar conservation laws*, Mathematics of Computation, 45 (1985), pp.15-21.
- [5] A. Harten, *High resolution schemes for hyperbolic conservation laws*, Journal of Computational Physics, 49 (1983), pp.357-393.
- [6] A. Harten, B. Engquist, S. Osher and S. Chakravarthy, *Uniformly high order accurate essentially non-oscillatory schemes, III*, Journal of Computational Physics, 71 (1987), pp.231-303.
- [7] G.-S. Jiang and C.-W. Shu, *On cell entropy inequality for discontinuous Galerkin methods*, Mathematics of Computation, 62 (1994), pp.531-538.
- [8] G.-S. Jiang and C.-W. Shu, *Efficient implementation of weighted ENO schemes*, Journal of Computational Physics, 126 (1996), pp.202-228.
- [9] P. Lax, *Hyperbolic systems of conservation laws II*, Communications on Pure and Applied Mathematics, 10 (1957), pp.537-566.
- [10] P. Lax, *Hyperbolic Systems of Conservation Laws and the Mathematical Theory of Shock Waves*, SIAM Regional Conference Series in Applied Mathematics, # 11, SIAM, Philadelphia, 1973.
- [11] R.J. LeVeque, *Numerical Methods for Conservation Laws*, Birkhauser Verlag, Basel, 1990.

- [12] X.-D. Liu and S. Osher, *Non-oscillatory high order accurate self similar maximum principle satisfying shock capturing schemes*, SIAM Journal on Numerical Analysis, 33 (1996), pp.760-779.
- [13] P.-L. Lions and P.E. Souganidis, *Convergence of MUSCL and filtered schemes for scalar conservation law and Hamilton-Jacobi equations*, Numerische Mathematik, 69 (1995), pp.441-470.
- [14] S. Osher and S. Chakravarthy, *Very high order accurate TVD schemes*, IMA Volumes in Mathematics and Its Applications, volume 2, Springer-Verlag, 1986, pp.229-274.
- [15] S. Osher and E. Tadmor, *On the convergence of the difference approximations to scalar conservation laws*, Mathematics of Computation, 50 (1988), pp.19-51.
- [16] R. Sanders, *A third-order accurate variation nonexpansive difference scheme for single nonlinear conservation law*, Mathematics of Computation, 51 (1988), pp.535-558.
- [17] C.-W. Shu, *TVB uniformly high order schemes for conservation laws*, Mathematics of Computation, 49 (1987), pp.105-121.
- [18] C.-W. Shu, *Essentially non-oscillatory and weighted essentially non-oscillatory schemes for hyperbolic conservation laws*, in *Advanced Numerical Approximation of Nonlinear Hyperbolic Equations*, B. Cockburn, C. Johnson, C.-W. Shu and E. Tadmor (Editor: A. Quarteroni), Lecture Notes in Mathematics, volume 1697, Springer, 1998, pp. 325-432.
- [19] B. van Leer, *Towards the ultimate conservative difference scheme V. A second order sequel to Godunov's method*, Journal of Computational Physics, v135 (1997), pp.229-248.
- [20] H. Yang, *Convergence of Godunov type schemes*, Applied Mathematics Letters, 9 (1996), pp.63-67.

- [21] H. Yang, *On wavewise entropy inequality for high-resolution schemes II: fully discrete MUSCL schemes with exact evolution in small time*, SIAM Journal on Numerical Analysis, 36 (1998), pp.1-31.